Complexation

DOI: 10.1002/ange.201103028

Selective *Endo* and *Exo* Binding of Alkali Metals to Corannulene**

*Sarah N. Spisak, Alexander V. Zabula, Alexander S. Filatov, Andrey Yu. Rogachev, and Marina A. Petrukhina**

The first report of complexation of a transition metal to corannulene in 1997[1] triggered intensive exploration of metal binding reactions to bowl-shaped polyaromatic hydrocarbons (buckybowls). Currently, buckybowls are known as multifunctional ligands in coordination chemistry.[2] They share with fullerenes a convex three-dimensional unsaturated carbon surface, but it is their open and sterically accessible concave face that makes buckybowls exceptional π ligands from a coordination viewpoint.[2,3] Studies of relative preferences of the convex (*exo*) and concave (*endo*) metal binding for buckybowls (Figure 1) have attracted considerable attention both theoretically[1,4] and experimentally[2] in the last few years. The recently reported remarkable examples of the drastically different reactivity of two closely related endohedral metallofullerene analogues[5] along with the enhanced catalytic efficiency of platinum nanoparticles embedded inside, rather than outside, carbon nanotubes[6] should further reinforce controlled preparation and investigation of the corresponding inclusion complexes of buckybowls.

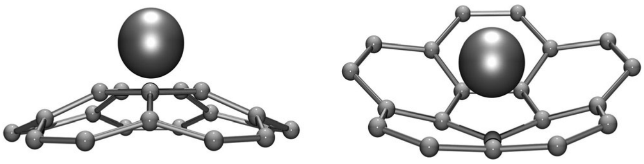

Figure 1. Representations of *exo* (left) and *endo* (right) binding modes.

To date, a number of complexes with different metal centers coordinated to corannulene have been isolated from solution reactions and structurally characterized. Several η^6 complexes with late transition metals (Ru, Os, Rh, Ir) indicate a strong preference of the convex surface of corannulene for coordination.[7] The solvent-free complexation reactions of corannulene and larger buckybowls with volatile electrophilic complexes of Rh^{II} and Ru^{I} result in the coordination of metal centers to the rim and spoke sites, as well as to a hub carbon atom of a π bowl.[8] All discrete complexes deposited from the gas phase also exhibit the preferential involvement of the convex corannulene surface in metal binding. For some time, these examples thwarted the idea of using buckybowls to access inclusion metal complexes. However in 2007, Hirao and co-workers achieved the first selective *endo* coordination of the FeCp unit to the concave face of sumanene ($C_{21}H_{12}$) in solution and in the solid state.[9] In contrast, the heavier RuCp unit exhibits both *exo* and *endo* coordination to sumanene in solution, but forms the *endo*-bound complex in the solid state.[10] Until now, the selective *endo* coordination has been unknown for corannulene.

Most recently, we have accomplished the first structural characterization of several surface-functionalized corannulene cations isolated as salts with $AlCl_4^-$.[11] Interestingly, the tight binding of the chlorine ends of $AlCl_4^-$ to the insides of the cationic bowls was observed in the solid state owing to complementary electrostatic interactions, which also illustrates the great ability of charged bowl-shaped polyaromatic containers for guest encapsulation. These data prompted us to investigate the complexation properties of corannulene anions with cations of main-group metals that may provide a good size fit (and thus enhanced dispersion interactions) with the concave cavity of the $C_{20}H_{10}^-$ bowl. While reduction reactions of corannulene ($C_{20}H_{10}$) with alkali metals have been broadly investigated in solution,[12] none of these species has been crystallographically characterized, thus providing additional stimulus in their structural analysis. As cesium and rubidium cations have the largest ionic radii of all non-radioactive metals (1.69 Å and 1.48 Å, respectively),[13] they were selected in this work as the most propitious candidates for *endo* binding.

The target product, $[Cs([18]crown\text{-}6)]^+[C_{20}H_{10}]^-$ (**1**), was prepared by reduction of corannulene with Cs (1.33 equiv) in the presence of [18]crown-6 in THF (Scheme 1).[14] The analogous reaction of $C_{20}H_{10}$ with Rb was impractical owing to a fast reduction of the desired monoanion to the purple corannulene dianion. However, $C_{20}H_{10}^{2-}$ generated in situ can be easily oxidized back to the monoanion by adding 1 equiv of neutral corannulene to afford $[Rb([18]crown\text{-}6)]^+[C_{20}H_{10}]^-$ (**2**). Both products **1** and **2** were isolated as dark green air- and moisture-sensitive solids in yields up to 85 %. Their composition and purity were confirmed by elemental analyses. The UV/Vis spectra for **1** and **2**, measured in THF, demonstrate slightly bathochromically shifted (up to 9 nm) absorbance maxima compared to $C_{20}H_{10}^-$, generated by the lithium reduction.[12d]

---

[*] S. N. Spisak, Dr. A. V. Zabula, Dr. A. S. Filatov,
Prof. Dr. M. A. Petrukhina
Department of Chemistry, University at Albany
State University of New York
Albany, NY 12222 (USA)
E-mail: marina@albany.edu
Dr. A. Y. Rogachev
Institute für Anorganische und Angewandte Chemie
Universität Hamburg (Germany)

[**] Financial support of this work from the National Science Foundation Career Award (CHE-0546945) is gratefully acknowledged. We also thank the University at Albany for supporting the X-ray center, and Dr. V. M. Grigoryants and C. Hauke for ESR and NMR measurements.

Supporting information for this article is available on the WWW under http://dx.doi.org/10.1002/anie.201103028.

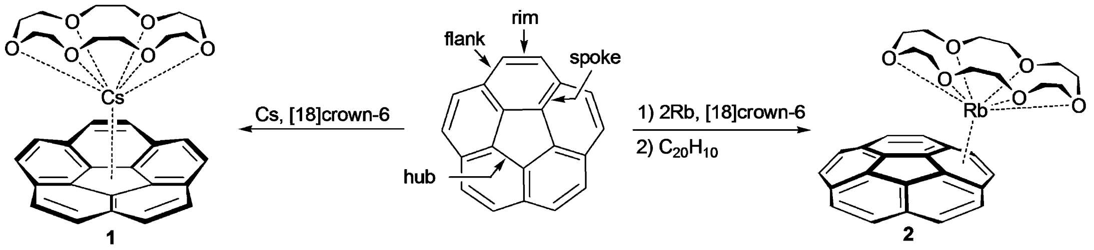

Scheme 1. Preparation of complexes **1** and **2**.

The variable-temperature ESR studies for the Li- and Na-doped corannulene monoanions in THF have been previously reported by Sato et al.[12h] The ESR signals ($g = 2.003$) for $C_{20}H_{10}^-$ with solvent-separated Li^+ or Na^+ cations at room temperature are composed of 11 equally spaced peaks. The ESR spectra become more complicated at low temperatures owing to the symmetry reduction of corannulene monoanions (Jahn–Teller effect).[12h]

The ESR signals ($g = 2.004$) for solutions of **1** and **2** at room temperature are more complex (Figure 2) than those observed for the monoanion with solvent-separated Li^+ and Na^+ ions under similar conditions. This may indicate that larger $[Rb([18]crown\text{-}6)]^+$ and $[Cs([18]crown\text{-}6)]^+$ ions are bound to the $C_{20}H_{10}^-$ bowl in solution. The ESR spectrum for **1** ($I = 7/2$ for ^{133}Cs) shows less splitting than that measured for **2** ($I = 5/2$ for ^{85}Rb and $I = 3/2$ for ^{87}Rb), suggesting that the corannulene anion in solution of **1** may exist in a more symmetrical environment than that in **2**.

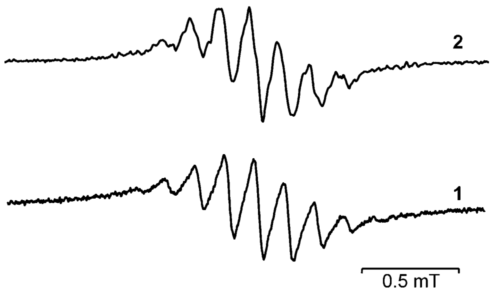

Figure 2. ESR spectra for **1** and **2** in THF at 25 °C.

The ^1H NMR study of crystals of **1** and **2** redissolved in $[D_8]THF$ revealed the presence of broad singlets for $[M([18]crown\text{-}6)]^+$ species in the range of $\delta = 3.9$–4.4 and 4.5–5.6 ppm, respectively, depending on the concentration and temperature. Such significantly downfield-shifted resonances, compared to the signals of diamagnetic $[M([18]crown\text{-}6)]^+$-containing salts ($\delta \approx 3.6$ ppm),[15] can be attributed to the paramagnetic shielding of the crown ether protons by the corannulene anion radical. This again illustrates that interaction of the $[M([18]crown\text{-}6)]^+$ moieties and $C_{20}H_{10}^-$ bowls persists in solution. The ^1H resonance signals of the [18]crown-6 ether in diluted solutions of **1** and **2** (ca. 1.5 mM) appear at $\delta = 3.7$ and 4.5 ppm, while in concentrated solutions (ca. 30 mM) these signals shift to $\delta = 4.2$ ppm (**1**) and $\delta = 5.3$ ppm (**2**), thus indicating a remarkable concentration dependence. Upon cooling of approximately 10 mM solutions of **1** and **2** in $[D_8]THF$ to −50 °C, the ^1H NMR resonance signals exhibit broadening and low-field shifts to $\delta = 4.4$ ppm for **1** and $\delta = 5.6$ ppm for **2**.[14]

Single crystals of **1** were grown from the diglyme solution by layering with hexanes at 10 °C. The X-ray diffraction study for **1** revealed an unprecedented *endo* binding of a metal to the corannulene bowl (Figure 3). The cesium cation bearing [18]crown-6 ether sits almost exactly above the center of the five-membered ring, thus representing the first example of η^5 binding for corannulene. The corresponding $Cs\cdots C_{hub}$ distances (3.424(3)–3.573(3) Å) are comparable with those measured in the π adducts having η^6- or η^5-bound cesium to planar polyaromatic hydrocarbons,[15,16] Cs-intercalated C_{60}-fullerene,[17] and fullerene nanopeapods.[18] The distance between the bottom of the $C_{20}H_{10}^-$ "dish" and the Cs^+ ion is 3.285(3) Å. Additional $Cs\cdots C$ contacts with interior walls of the corannulene bowl fall in the range of 3.616(3)–3.899(3) Å, while the separations from the rim carbon atoms are 3.900(3)–4.230(3) Å. Owing to its large size, Cs^+ does not fit inside the [18]crown-6 ring. The $Cs\cdots O$ bonds (3.139(2)–3.216(2) Å) are close to those previously reported for $[Cs([18]crown\text{-}6)]^+$-containing salts with planar aromatic systems.[15,16]

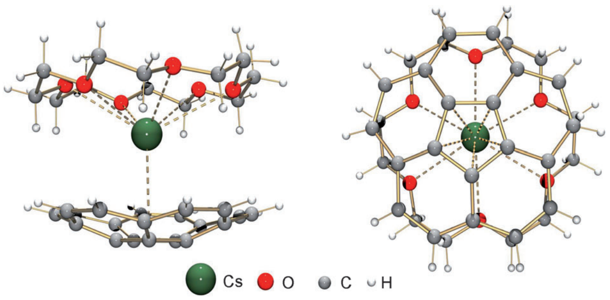

Figure 3. Orthogonal views of the molecular structure of **1**.

In the corannulene anion, the observed slight shortening of the hub C−C bonds (av. 1.403(4) Å) compared to the parent bowl (av. 1.415(2) Å)[19] can be considered insignificant from the crystallographic point of view. The spoke C−C bonds are longer in the monoanion than in the neutral corannulene (av. 1.412(4) Å vs. 1.379(2) Å). Notably, the flank C−C bonds (av. 1.423(4) Å vs. 1.446(2) Å) are shortened, while the rim bonds are elongated (av. 1.410(4) Å vs. 1.383(2) Å) upon one-electron reduction. This bond length adjustment indicates greater delocalization of π electrons in the outer 15-membered ring of the monoanion in comparison with that of the neutral corannulene. Interestingly, all these geometrical perturbations do not cause a significant flattening of $C_{20}H_{10}^-$ (bowl depth 0.846(4) vs. 0.875(2) Å for $C_{20}H_{10}$).[19] The space-filling model (Figure 4, left) demonstrates that the cesium ion is perfectly "dished-up" in the monoanionic corannulene bowl. The comparable diameters of the [Cs([18]crown-6)]$^+$ (9.1 Å) and corannulene anion (8.3 Å) moieties facilitate a compact packing of **1** in the crystal (Figure 4, right).

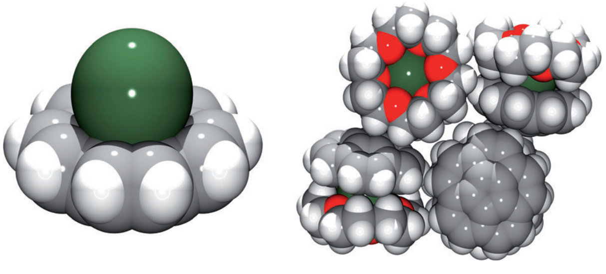

Figure 4. Space-filling models for Cs$^+$ with a corannulene anion (left) and the solid-state packing of **1** (right).

Single crystals of **2** were grown from the 1,2-dimethoxyethane solution layered with hexanes at 10 °C as a mixture of dark-green plates (**2a**) and blocks (**2b**). According to the X-ray diffraction studies, **2** crystallizes as discrete monomeric species in **2a**, whereas it forms a 1D polymer in the solid state structure of **2b** (Figure 5). In contrast to an *endo* metal coordination in **1**, the [Rb([18]crown-6)]$^+$ unit shows selective *exo* binding to the corannulene monoanion in both **2a** and **2b**.

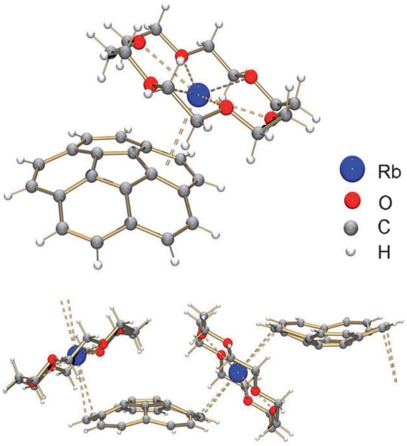

Figure 5. The molecular structure of **2a** (top) and the fragment of a 1D polymer of **2b** (bottom).

In **2a**, the rubidium ion is located above the six-membered ring of the monoanion, similarly to the η^6-coordination previously seen in several transition metal complexes of corannulene.[7] The Rb–C bonds (3.273(3)–3.479(3) Å) as well as the distance of Rb$^+$ to the centroid of the six-membered ring of $C_{20}H_{10}^-$ (3.040(3) Å) are indicative of rather strong metal binding to the π bowl. The hub and flank C–C bonds (av. 1.413(3) Å and 1.440(3) Å, respectively) remain essentially unchanged in the $C_{20}H_{10}^-$ anion of **2a** compared to the neutral corannulene (1.415(2) Å and 1.446(2) Å), whereas the spoke and rim C–C bonds become slightly elongated (av. 1.397(3) Å and 1.395(3) Å vs. 1.379(2) Å and 1.383(2) Å). The corannulene bowl depth in **2a** is 0.862(3) Å. This demonstrates that the encapsulation of Cs$^+$ inside the $C_{20}H_{10}^-$ anion in **1** causes slightly stronger deformation of the polyaromatic bowl than the outside binding of Rb$^+$ in **2a**. Overall, despite following the same trends in perturbation of the corannulene core geometry upon one-electron reduction, the imposed changes in the case of Rb$^+$ are notably less pronounced compared to Cs$^+$.

In **2b**, the corannulene monoanions are linked together by [Rb([18]crown-6)]$^+$ ions into 1D polymeric chains. The steric repulsion of the crown ether fragments prevents the η^6 binding of the rubidium ions and forces both [Rb([18]crown-6)]$^+$ moieties to the edge of $C_{20}H_{10}^-$ in the crystal lattice of **2b**. The positional disorder of the corannulene core in **2b** precludes the precise inspection of its geometrical parameters.

To shed more light on the strength of interactions and preferable binding modes of alkali metals to corannulene, we carried out theoretical calculations for **1**, **2**, and their potassium analogue (**3**) at the DFT//PBE0 level of theory using triple-zeta basis sets 6-311G(d,p) (for C, H, O) and def2-TZVP (for K, Rb, Cs).[14] Density functional calculations closely reproduced the X-ray structures of **1** and **2** and revealed the presence of three minima on the potential energy surfaces corresponding to the isomers with different binding of metal units for **1**–**3**. Complexes **1**–**3** can exist as an *endo* (**I**, Figure 6a) isomer and the two *exo* isomers, showing the binding of an alkali metal to the benzene ring (η^6, **II**, Figure 6b) or to the central five-membered ring (η^5, **III**, Figure 6c) of the corannulene anion.

As can be seen from Table 1, the concave binding is favored for [Cs([18]crown-6)]$^+$ only and the stability of the *endo*-bound species decreases on going from Cs$^+$ to K$^+$. An opposite trend is found for the *exo* binding in isomers **II** and **III**, which seems favorable for K$^+$ and Rb$^+$ ions. For the

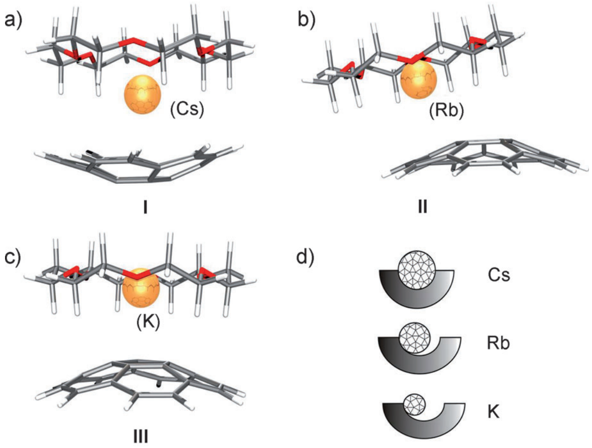

Figure 6. a)–c) Optimized geometries for **I**–**III** (only one isomer is shown for each metal) and d) representation of the arrangement of an alkali metal inside the bowl in **I**.

Table 1: Relative energies[a] for models **I**–**III** from DFT calculations.

	I (*endo*)	**II** (*exo* η^6)	**III** (*exo* η^5)
Cs	0.00	+2.33	+3.15
Rb	+3.12	+1.55	0.00
K	+7.90	+2.84	0.00

[a] The energy estimations [kcal mol^{-1}] are related to the lowest-energy isomer for each metal.

isomers of type **I**, only the Cs^+ ion is found to sit symmetrically inside the $C_{20}H_{10}^-$ bowl (Figure 6d). It can be explained by an almost ideal geometrical match between the sizes of the cesium cation and the *endo* cavity of corannulene ("the ball and socket" model). This results in equal interaction of Cs^+ with all five rim bonds and the whole concave surface of $C_{20}H_{10}^-$. As there is no such "ideal match" between the sizes of K^+ and Rb^+ ions and the concave surface of corannulene, these metals tend to shift towards one of the rim bonds of $C_{20}H_{10}^-$ in their *endo*-bound isomers.

It is worth mentioning that owing to the well-established deficiency of DFT approaches (even in the hybrid variant) in description of dispersion forces, the small difference in energy found between the η^5- and η^6-*exo* isomers should be accepted with care. However, the theoretical results correctly predict different *endo*/*exo* binding preferences for Cs^+ and Rb^+ and are in agreement with our experimental observations on selective binding of these close alkali metal relatives to corannulene. It should be mentioned that incorporation of [18]crown-6 ether moiety into calculations is required to observe the correct trend, as even very recent DFT calculations of buckybowl complexes that used "naked" alkali metal cations[20] did not conform to the experimentally observed results.

In conclusion, we have successfully isolated the cesium and rubidium salts of the corannulene monoanion in the single crystalline form and reported the first structural characterization of the $C_{20}H_{10}^-$ bowl. The Cs^+ cation was found to be centrally bound to the concave surface of the bowl, rendering the first example of the concave corannulene product. The smaller Rb^+ ion selectively coordinates to the bowl outside in both crystallographically characterized compounds, experimentally confirming that the site preference of alkali metal binding to corannulene depends on the ion size. The broad investigation of corannulene anions prepared by multiple electron reduction reactions with other alkali and alkaline earth metals is currently underway.

Received: May 2, 2011

Keywords: alkali metals · carbanions · coordination modes · corannulenes · X-ray diffraction

---

[1] T. J. Seiders, K. K. Baldridge, J. M. O'Connor, J. S. Siegel, *J. Am. Chem. Soc.* **1997**, *119*, 4781–4782.

[2] A. S. Filatov, M. A. Petrukhina, *Coord. Chem. Rev.* **2010**, *254*, 2234–2246.

[3] M. A. Petrukhina, *Angew. Chem.* **2008**, *120*, 1572–1574; *Angew. Chem. Int. Ed.* **2008**, *47*, 1550–1552.

[4] a) M. V. Frash, A. C. Hopkinson, D. K. Bohme, *J. Am. Chem. Soc.* **2001**, *123*, 6687–6695; b) F. Nunzi, A. Sgamellotti, N. Re, *Organometallics* **2002**, *21*, 2219–2225; c) R. C. Dunbar, *J. Phys. Chem. A* **2002**, *106*, 9809–9819; d) U. D. Priyakumar, G. N. Sastry, *Tetrahedron Lett.* **2003**, *44*, 6043–6046; e) Y. Kameno, A. Ikeda, Y. Nakao, H. Sato, S. Sakaki, *J. Phys. Chem. A* **2005**, *109*, 8055–8063; f) M. W. Stoddart, J. H. Brownie, M. C. Baird, H. L. Schmider, *J. Organomet. Chem.* **2005**, *690*, 3440–3450; g) A. Yu. Rogachev, M. A. Petrukhina, *J. Phys. Chem. A* **2009**, *113*, 5743–5753.

[5] F.-F. Li, A. Rodríguez-Fortea, J. M. Poblet, L. Echegoyen, *J. Am. Chem. Soc.* **2011**, *133*, 2760–2765.

[6] Z. Chen, Z. Guan, M. Li, Q. Yang, C. Li, *Angew. Chem.* **2011**, *123*, 5015–5019; *Angew. Chem. Int. Ed.* **2011**, *50*, 4913–4917.

[7] a) P. A. Vecchi, C. M. Alvarez, A. Ellern, R. J. Angelici, A. Sygula, R. Sygula, P. W. Rabideau, *Angew. Chem.* **2004**, *116*, 4597–4600; *Angew. Chem. Int. Ed.* **2004**, *43*, 4497–4500; b) J. S. Siegel, K. K. Baldridge, A. Linden, R. Dorta, *J. Am. Chem. Soc.* **2006**, *128*, 10644–10645; c) B. Zhu, A. Ellern, A. Sygula, R. Sygula, R. J. Angelici, *Organometallics* **2007**, *26*, 1721–1728; d) D. Bandera, K. K. Baldridge, A. Linden, R. Dorta, J. S. Siegel, *Angew. Chem.* **2011**, *123*, 895–897; *Angew. Chem. Int. Ed.* **2011**, *50*, 865–867.

[8] a) M. A. Petrukhina, K. W. Andreini, J. Mack, L. T. Scott, *Angew. Chem.* **2003**, *115*, 3497–3501; *Angew. Chem. Int. Ed.* **2003**, *42*, 3375–3379; b) M. A. Petrukhina, L. T. Scott, *Dalton Trans.* **2005**, 2969–2975; c) M. A. Petrukhina, Y. Sevryugina, A. Yu. Rogachev, E. A. Jackson, L. T. Scott, *Angew. Chem.* **2006**, *118*, 7366–7368; *Angew. Chem. Int. Ed.* **2006**, *45*, 7208–7210; d) M. A. Petrukhina, Y. Sevryugina, A. Yu. Rogachev, E. A. Jackson, L. T. Scott, *Organometallics* **2006**, *25*, 5492–5495; e) A. S. Filatov, A. Yu. Rogachev, E. A. Jackson, L. T. Scott, M. A. Petrukhina, *Organometallics* **2010**, *29*, 1231–1237.

[9] a) T. Amaya, H. Sakane, T. Hirao, *Angew. Chem.* **2007**, *119*, 8528–8531; *Angew. Chem. Int. Ed.* **2007**, *46*, 8376–8379; b) H. Sakane, T. Amaya, T. Moriuchi, T. Hirao, *Angew. Chem.* **2009**, *121*, 1668–1671; *Angew. Chem. Int. Ed.* **2009**, *48*, 1640–1643.

[10] T. Amaya, W.-Z. Wang, H. Sakane, T. Moriuchi, T. Hirao, *Angew. Chem.* **2010**, *122*, 413–416; *Angew. Chem. Int. Ed.* **2010**, *49*, 403–406.

[11] A. V. Zabula, S. N. Spisak, A. S. Filatov, A. Yu. Rogachev, M. A. Petrukhina, *Angew. Chem.* **2011**, *123*, 3027–3030; *Angew. Chem. Int. Ed.* **2011**, *50*, 2971–2974.

[12] a) J. Janata, J. Gendell, C.-Y. Ling, W. Barth, L. Backs, H. B. Mark, Jr., R. G. Lawton, *J. Am. Chem. Soc.* **1967**, *89*, 3056–3058; b) A. Ayalon, M. Rabinovitz, P.-C. Cheng, L. T. Scott, *Angew. Chem.* **1992**, *104*, 1691–1692; *Angew. Chem. Int. Ed. Engl.* **1992**, *31*, 1636–1637; c) A. Ayalon, A. Sygula, P.-C. Cheng, M. Rabinovitz, P. W. Rabideau, L. T. Scott, *Science* **1994**, *265*, 1065–1067; d) M. Baumgarten, J. L. Gherghel, M. Wagner, A. Weitz, M. Rabinovitz, P.-C. Cheng, L. T. Scott, *J. Am. Chem. Soc.* **1995**, *117*, 6254–6257; e) A. Weitz, M. Rabinovitz, P.-C. Cheng, L. T. Scott, *Synth. Met.* **1997**, *86*, 2159–2160; f) A. Weitz, E. Shabtai, M. Rabinovitz, M. S. Bratcher, C. C. McComas, M. D. Best, L. T. Scott, *Chem. Eur. J.* **1998**, *4*, 234–239; g) R. Shenhar, I. Willner, D. V. Preda, L. T. Scott, M. Rabinovitz, *J. Phys. Chem. A* **2000**, *104*, 10631–10636; h) T. Sato, A. Yamamoto, H. Tanaka, *Chem. Phys. Lett.* **2000**, *326*, 573–579; i) I. Aprahamian, D. Eisenberg, R. E. Hoffman, T. Sternfeld, Y. Matsuo, E. A. Jackson, E. Nakamura, L. T. Scott, T. Sheradsky, M. Rabinovitz, *J. Am. Chem. Soc.* **2005**, *127*, 9581–9587; j) D. Eisenberg, J. M. Quimby, E. A. Jackson, L. T. Scott, R. Shenhar, *Chem. Commun.* **2010**, *46*, 9010–9012.

[13] H. Bock, K. Ruppert, *Inorg. Chem.* **1992**, *31*, 5094–5099.

[14] See the Supporting Information for detailed synthetic procedures, characterization, X-ray diffraction studies, and theoretical calculations.

[15] a) S. Neander, U. Behrens, F. Olbrich, *J. Organomet. Chem.* **2000**, *604*, 59–67; b) I. Heldt, U. Behrens, *Z. Anorg. Allg. Chem.* **2005**, *631*, 749–758.

[16] H. Bock, T. Hauck, C. Näther, *Organometallics* **1996**, *15*, 1527–1529.

[17] O. Zhou, J. E. Fischer, N. Coustel, S. Kycia, Q. Zhu, A. R. McGhie, W. J. Romanow, J. P. McCauley, Jr., A. B. Smith III, D. E. Cox, *Nature* **1991**, *351*, 462–464.

[18] Y. Sato, K. Suenaga, S. Bandow, S. Iijima, *Small* **2008**, *4*, 1080–1083.

[19] a) J. C. Hanson, C. E. Nordman, *Acta Crystallogr. Sect. B* **1976**, *32*, 1147–1153; b) M. A. Petrukhina, K. W. Andreini, J. Mack, L. T. Scott, *J. Org. Chem.* **2005**, *70*, 5713–5716.

[20] a) J. A. Carrazana-García, J. Rodriguez-Otero, E. M. Cabaleiro-Lago, *J. Phys. Chem. B* **2011**, *115*, 2774–2782; b) J. R. Green, R. C. Dunbar, *J. Phys. Chem. A* **2011**, *115*, 4968–4975.